International Journal of Advanced Structural Engineering, Vol. 1, No. 1, Pages 77-92, July 2009
Islamic Azad University, South Tehran Branch

# HYSTERETIC DISSIPATORS MADE OF ALUMINIUM AND STEEL: OPTIMAL DESIGN AND PRELIMINARY CHARACTERIZATION TESTS

Mariella Diaferio[1], Dora Foti[2] and Riccardo Nobile[3]
[1, 2] *Department of Civil and Environmental Engineering, Politecnico die Bari, Bari, Italy*
[3] *Department of Innovation Engineering, Università del Salento, Lecce, Italy*

Received 11 January 2009
Revised 18 February 2009
Accepted 20 March 2009

In this paper the optimal design of a dissipator made of aluminium and steel and principally subjected to shear forces and the preliminary results of the characterization tests are described. The device has been designed on the basis of an optimization procedure with the objective to maximize the energy dissipated in the device. The response of a 3D frame equipped with the device and subjected to 7 earthquakes compatible with the response spectrum of Eurocode 8 is shown. The optimal response obtained from the characterization tests exhibits a good dissipative behavior of the device, highlighted by a wide enough hysteresis cycle.

*Keywords:* Passive control, yielding-based device, design optimization, non-linear dynamic analysis.

## 1. Introduction

In the field of seismic passive protection of structures an important role is given to hysteretic devices that produce a reduction of the energy entering the building thanks to the plastic behavior of the material. In particular, metallic devices show a stable behavior under cyclic loads, producing a wide hysteresis cycle which depends on the yielding limit of the material. An example of these devices is represented by steel panels subjected to shear force. Usually such devices possess a wide dissipative capacity related to their dimensions. The introduction of such devices in the building produces an increment of the stiffness of the structure and a reduction of

[1] Assistant Professor
[2] Professor
[3] Assistant Professor

the inter-story drifts, concentrating the damage in the device. The limit of these kinds of Energy Dissipating Devices is that the dissipation capacity is activated only after they sustain large excursions in the inelastic field. As consequence, the devices are ineffective for vibrations smaller than the inter-story drift that produces the yielding of the material composing the device.

To reduce the displacement in correspondence of which the hysteresis cycles of the dissipators are activated, Nakashima et al. (1994), Nakashima(1995) and Yamaguchi et al. (1998) proposed the use of low-yield steel (LYS) to build dissipators with a shear behavior. Nevertheless, the costs and the not easy availability of low-yield steel pushed the research towards alternative but similar materials, such as aluminium (Rai and Wallace 1998, Foti and Diaferio 1999 and Foti and Nobile 2000). In fact, aluminum is characterized by a low yielding force, lower than the LYS one, and a wide plastic field. In Rai and Wallace (1998) and Foti et al. (1999 and 2000) hysteretic devices made with ordinary aluminium alloys have been proposed and the results of numerical and experimental investigations are shown. De Matteis et al. (2007) proposed the use of pure aluminium for hysteretic dissipators.

In the present paper the optimal design of a shear panel made of aluminium and steel and the results of preliminary characterization tests are shown. The dimensions of the device have been determined in order to maximize the hysteretic energy dissipation . Then the response of a 3D frame equipped with the aforementioned devices and subjected to 7 earthquakes compatible with the response spectrum of Eurocode 8 for type A soil in seismic zone 1 is shown.

Finally, the preliminary experimental results obtained from the characterization tests on the device are shown. By mean of the interpolation of the experimental results, some analytical expressions of the applied shear load and the maximum displacement measured at the top of the panel have been determined for the device.

## 2. Aluminium-Steel Shear Panel

Shear panels could dissipate a large amount of energy when two conditions are satisfied. The first is that inelastic excursions are activated in correspondence of a low yielding limit that could guarantee the protection of the structure even in the range of small vibrations; the second is that they show a wide plastic range. These two peculiarities give contrasting requirements: the reduction of the yielding limit implies a reduction of the dimensions of the device and, on the other side, the request of a wide plastic range needs an increment of some dimensions of the device, in order to increase the shear buckling threshold, and, as a consequence, to avoid the possibility of an out-of-plane instability of the device. On the basis of the above mentioned considerations, the proposed device has been designed as composed by three plates: the central

plate, preferentially devoted to the energy dissipation, and two external plates, with the main aim of reducing the possibility of out-of-plane instability (Figure 1). In particular, Fe360 steel has been chosen for the external plates and 1000 aluminium alloy has been chosen for the web of the device. The choice of the aluminium alloy is due to its low yielding stress and its wide plastic range. In Table 1 the mechanical properties of the two materials are described.

Table 1. Steel and aluminium mechanical properties

| | Material properties | Fe360 | 1000 Al series |
|---|---|---|---|
| $\sigma_y$ | yielding stress [N/mm$^2$] | 235 | 30 |
| $\sigma_R$ | ultimate tensile strength [N/mm$^2$] | 360 | 90 |
| A | elongation to failure [%] | 26 | 40 |
| E | Young's modulus [N/mm$^2$] | 206000 | 70000 |
| H | Plastic modulus [N/mm$^2$] | 20000 | 5000 |

The steel plates present some rectangular openings where the central aluminium plate partly emerges into the steel; in this way, the steel openings represent an obstacle to slip phenomena. Moreover, bolts have been considered to guarantee a better connection between the plates. In order to increase the buckling threshold, the steel plates are oriented with their higher inertia in the direction of the out-of-plane instability. A typical configuration of the panel is shown in Figure 1.

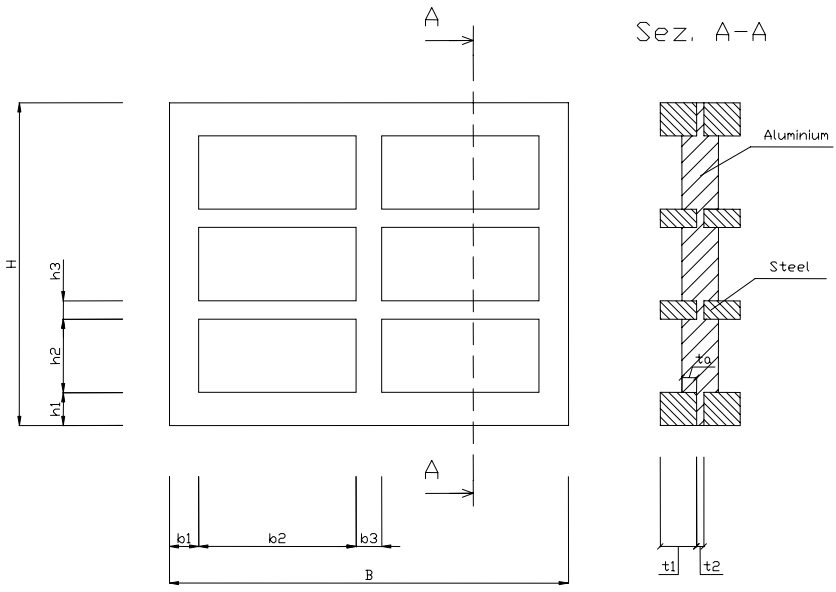


Figure 1. Geometrical parameters of the aluminium- steel shear panel

An optimization analysis has been carried out to define the geometrical configuration of the device by means of ANSYS software. The panel has been modelled using 20-nodes solid

elements SOLID90 having a parabolic shape function. The mechanical behaviors of steel and aluminium have been described by bi-linear laws, whose parameters were defined in accordance with the properties shown in Table 1. Moreover, the shear panel has been modelled as fixed at the base and able to move only in the horizontal direction at the upper bound. The assumed constraints have been adopted in order to simplify the installation of the device in the structure. In particular, the device could be welded or connected with some bolts at the base and at the upper bound.

The geometrical shapes and dimensions of the aluminium-steel shear panel have been determined by imposing a maximum horizontal displacement equal to 4 mm, that is 0.2% of the inter-story height of the steel frame described in chapter 3, where the proposed device will be installed and subjected to shaking-table tests (Ponzo et al. 2007). An optimization procedure for a FE model of the device has been applied. It essentially consists of the following steps:

- Individuation of the objective function to be maximized;
- Declaration of the parameters that define the geometry of the device;
- Definition of the variability ranges of the parameters, in order to exclude unrealistic solutions;
- Individuation of constraint functions.

The objective function to maximize has been chosen equal to the plastic strain energy in the aluminium plate. In Figure 1, the main geometrical parameters needed to define the device configuration are shown. The optimal design has been performed by assuming the ranges for the parameters of the aluminium-steel device and the starting configuration resumed in Table 2.

Table 2. Starting configuration and variability ranges of the parameters of the aluminium-steel device

| | Geometrical Parameters | Starting Configuration | Variability range |
|---|---|---|---|
| $n_x$ | horizontal openings | 6 | 2-6 |
| $n_y$ | vertical openings | 4 | 1-4 |
| $b_1$ | lateral steel stiffener width [mm] | 20 | 5-20 |
| $b_2$ | aluminium opening width [mm] | 60 | 20-200 |
| $b_3$ | internal steel stiffener width [mm] | 20 | 5-20 |
| $h_1$ | external steel stiffener height [mm] | 20 | 5-20 |
| $h_2$ | aluminium opening height [mm] | 70 | 20-400 |
| $h_3$ | internal steel stiffener height [mm] | 20 | 5-20 |
| $t_1$ | steel plate thickness [mm] | 1 | 1-10 |
| $t_2$ | aluminium plate thickness [mm] | 3 | 1-4 |
| $t_a$ | aluminium opening projection [mm] | 2.5 | 1-4 |

Finally, correct formulation of the optimization procedure requires the following different constraint functions: maximum stress = 90 MPa; panel height = 380-450 mm; panel width = 150-

600 mm. Such constraints have been defined on the basis of geometrical considerations on the installation of the devices in the two-story steel frame described in chapter 3. The optimization routine has been performed by fixing *a priori* many configurations of the device, each one characterized by certain fixed numbers of the vertical and horizontal openings. The final results would be an optimized solution for each configuration; among them it would be easy to find the best configuration.

The optimization analysis has been performed by assuming that the aluminium plate is thicker than the steel one (Diaferio et al. 2008); on the contrary, in the present paper the optimization procedure has been performed to evaluate the dimensions of an aluminium-steel device characterized by steel plates with thickness higher than the aluminium plate. In fact, the analysis has shown that, even in the case of devices with the same yielding force, the dissipator with a thickness of the steel plates higher than the aluminium plate shows an almost uniform plasticization of the aluminium plate (Figure 2a): this could improve the dissipative capacities of the device. Thus, in the present paper, the dynamical analysis has been performed adopting the last solution and the dimensions reported in Figure 2. In particular, the Von Mises strain and the constitutive law of the proposed shear panel are shown.

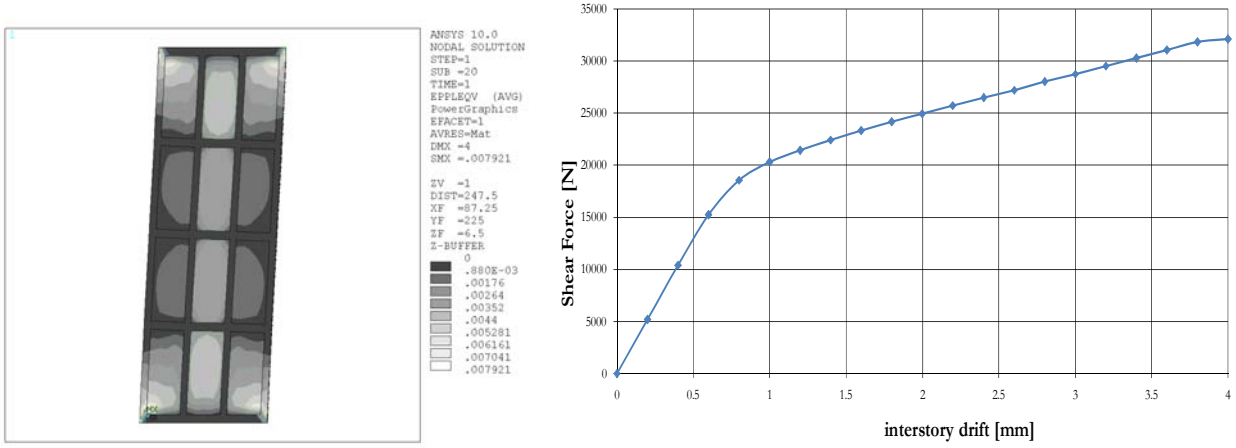


(a) (b)

Figure 2. Aluminium - steel device with 12 windows ($n_x$ 3 and $n_y$ 4) and $b_1$= 8mm, $b_2$=40mm, $b_3$=8mm, $h_1$=10mm, $h_2$=100mm, $h_3$=10mm, $t_1$=5mm, $t_2$=3mm, $t_a$=2mm: a) Von Mises strain; b) Constitutive law

## 3. Test Specimen

The shear panel has been proposed within the Research Project No. 7 of 2005-2008 ReLuis Project (Ponzo et al. and Serino et al. and Gattulli et al. 2007) whose scope is to conduct analytical and experimental investigations on seismic control techniques. The research project

foresees shaking-table tests on a 3D two-storey steel frame that has been build at the Structural Engineering Laboratory of the University of Basilicata in Potenza (Ponzo and Serino et al. 2007).

The specimen represents a 2:3 scaled steel frame; it has 3m x 4m plan size and presents four HEB140 columns placed at the corners and IPE180 beams welded to the columns. The storey height is about 2 m, and the columns emerge of 0.5m from the upper floor (Figure 3). The two floors are realized with concrete slabs supported by an A55/P600 coffer steel section with a thickness of 0.8mm. Moreover, HEA160 horizontal bracings are mounted in the plane of the ground floor. The frame is also equipped with chevron type bracings made of HEA100 mounted in the vertical planes (Figure 3c) and good to install the seismic protection devices. In detail, the proposed devices will be bolted at the base to the chevron bracings and at the upper bound of the beam. In this way, all rotations at the boundaries could be neglected.

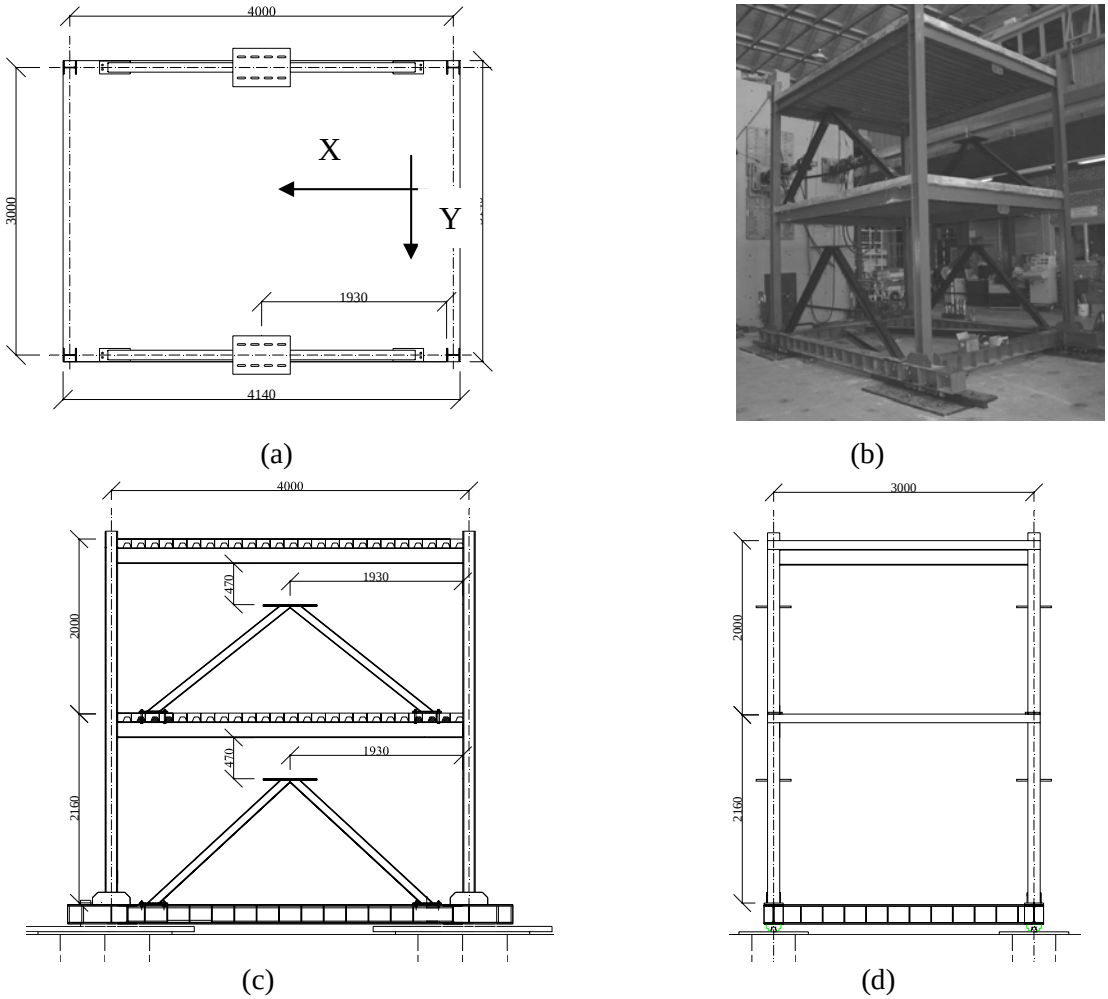


Figure 3. 2:3 scaled steel frame built at the Structural Engineering Laboratory of the University of Basilicata in Potenza, Italy: a) Plan view; b) 3D view; c) Vertical plane XZ; d) Vertical plane YZ

The installation of the aluminium-steel device in the structures will be realized introducing into the frame chevron type bracings, at the end of which a plate will be welded. In this way, the aluminium-steel panel will be fixed by bolts at the lower bound to the plate welded at the end of the chevron type bracings and at the upper bound to the beam of the structure (Figure 4). It is obvious that the dimensions of the shear panel must be adapted to the structure on which the device will be mounted on. Just to fix the idea, it has been assumed that the proposed device has to be installed in a frame similar to the one that will be used within the Reluis research project. Such dimensions have been chosen in order to utilize the proposed design procedure also to define the optimal device for the seismic protection of the aforementioned 3D steel frame (Figure 3).

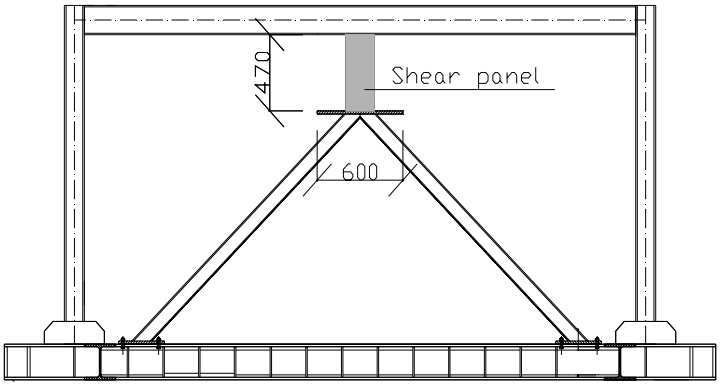


Figure 4. Location of the aluminium-steel device in the structure

## 4. Dynamic Performance of the Aluminium-Steel Device

The aim of the current non-linear dynamical analysis is to analyze the beneficial effects of one of the proposed aluminium – steel device introduced in the above mentioned 3D steel frame. Numerical results have been obtained by means of SAP 2000 Nonlinear ®.

The analysis has been performed modeling the devices as nonlinear links with the constitutive law of Figure 2b. The non-linear dynamical analysis has been performed subjecting the steel frame with (protected frame) and without (bare frame) aluminium-steel dissipators to 7 natural earthquakes, acting in the X direction. In particular, the 7 earthquakes (see Figure 5) are compatible with the response spectrum provided by Eurocode 8 for type A soil in seismic zone 1 and they are characterized by a seismic intensity equal to 0.35g (Serino et al. 2007 )

In Table 3 the modal frequencies of the bare and protected frames are shown. As a consequence of the installation of the aluminium-steel dissipators, the frequencies of the bending modes in the

X direction – i.e. the effective direction of the devices – and of the torsional modes significantly increase.

The global damage index – defined as the ratio of the top displacement on the total height of the frame – is shown in Figure 6. The results show that the response of the protected frame is three or four times smaller than the one of the bare frame and, in all the examined cases, no plasticization occurs in the frame.

In order to emphasize the effects of aluminium-steel dampers, the maximum inter-story drift index has been evaluated for each one of the 7 earthquakes. The above mentioned index is defined as the ratio of the maximum inter-story drift on the story height. In Figure 7 the indexes evaluated at each floor are represented. It is shown that for all the examined cases, the response of the protected frame satisfies the recommendation that the index must not exceed the limit of 0.5%, that is the security limit estimated with reference to the first plasticization of the frame (Ponzo et al. 2007).

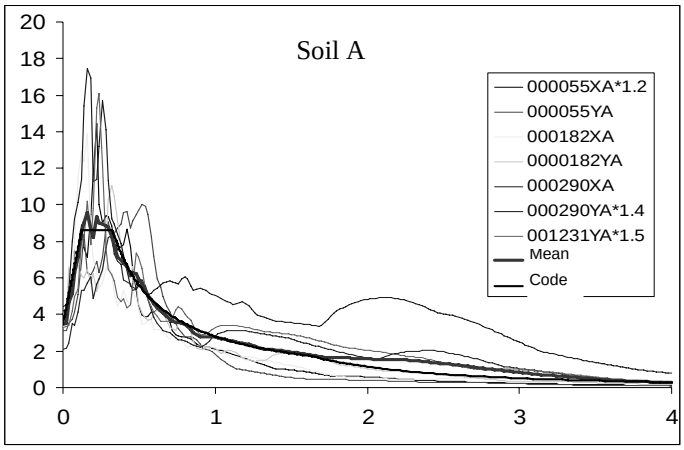


Figure 5. Response spectrum of the considered natural earthquakes compatible with Eurocode 8 for type A soil in seismic zone 1, PGA=0.35g

Table 3. Modal frequencies of the bare and protected frame

| Mode | Bare frame frequency [Hz] | Protected frame frequency [Hz] |
|---|---|---|
| I bending Y direction | 2.86 | 2.91 |
| I bending X direction | 3.56 | 10.64 |
| I torsion | 5.79 | 12.46 |
| II bending Y direction | 9.18 | 9.16 |
| II bending X direction | 12.53 | 29.14 |
| II torsion | 18.56 | 34.21 |

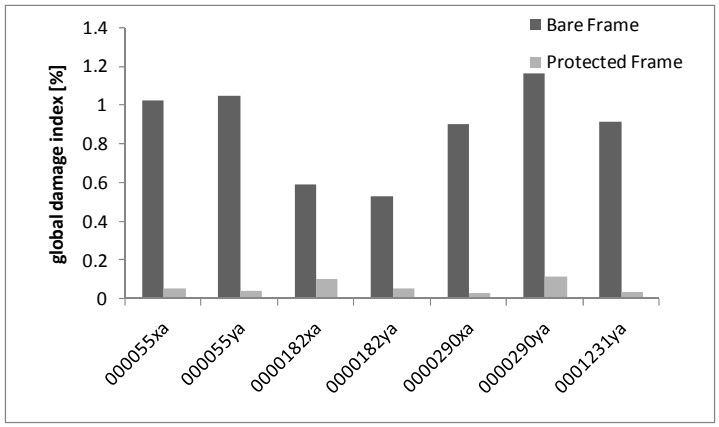


Figure 6. Global damage index for earthquakes compatible with Eurocode 8 for type A soil in seismic zone 1, PGA=0.35g

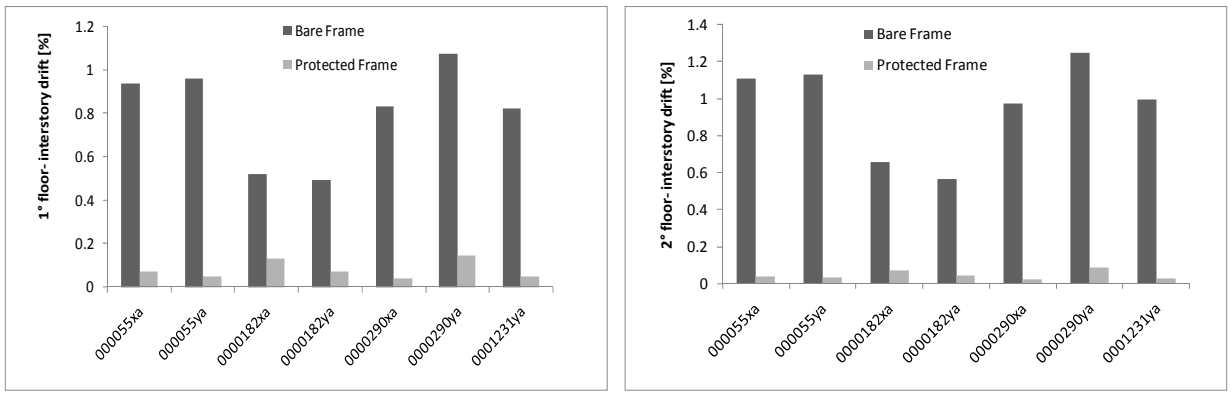


(a) (b)

Figure 7. Maximum inter-story drift index: earthquakes compatible with Eurocode 8 for type A soils in seismic zone 1, PGA=0.35g a) 1° floor and b) 2° floor

## 5. Device Mechanical Characterization

On the basis of the optimization analysis the final configuration and the constructive details of the panel are shown in Figure 8. The device has been subjected to tests with the load applied at the top and acting in the plane of the panel itself, with an intensity varying in the time.

The test set-up has been designed according to the working conditions of the panels in the 3D frame described before. In particular, a steel frame composed of a beam at the base (HEB 120), two vertical elements (HEB120) and a top beam (HEB 120). In the middle of the last beam, a 250 KN Enerpac actuator has been connected. It can apply a linear variable load to a couple of panels, installed in the frame as shown in Figure 9. As a consequence, the load transmitted to the actuator is equally divided in the two panels, even if distortions and misalignments are present. A type

TC4 load cell of AEP (Modena), with a maximum load of 100 kN, has been mounted on the top of the actuator in order to measure the applied load (Figure 10b). The panels are fixed at the columns by means of bolts with the same modalities expected for the 3D frame, while at the top, due to the symmetry of the testing system, the panels are only subjected to vertical displacements.

The tests have been performed at the Laboratory "M. Salvati" of the Department of Civil and Environmental Engineering of the Technical University of Bari.

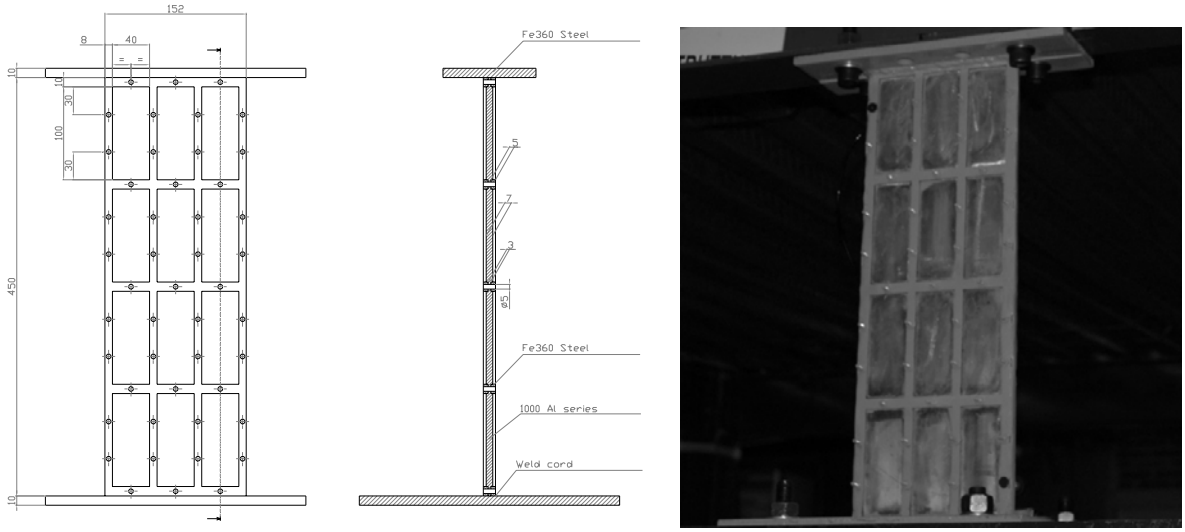


Figure 8. Constructive details of the device

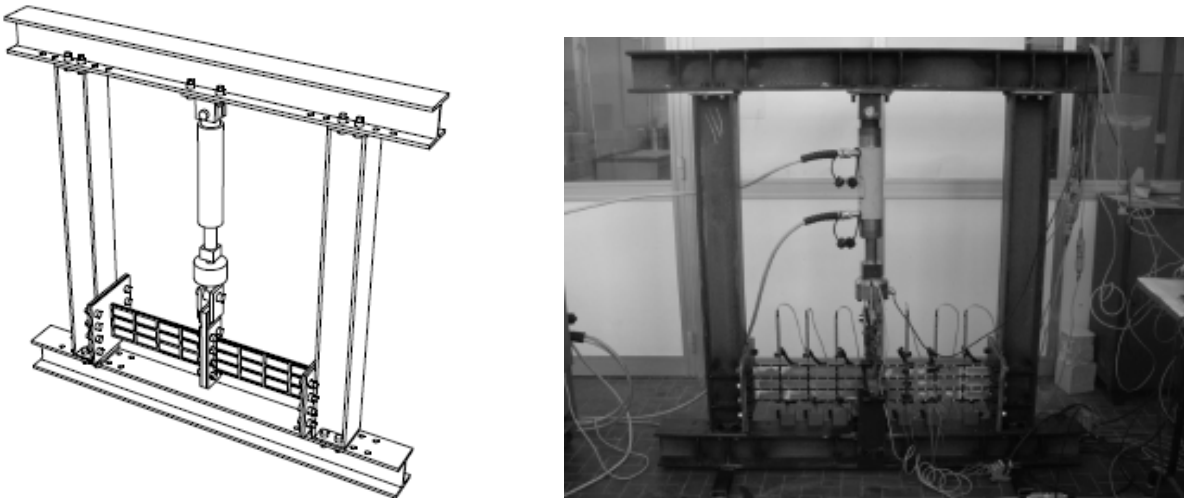

Figure 9. Testing set-up

During the tests, displacements have been measured at some points of the panels, chosen on the horizontal free edges and at the point of application of the load. The displacements have been measured by 8 transducers LVDT with a stroke equal to 10 mm and accuracy <0.10% (Figure 10a). It has been possible to determine the force-displacement diagram described in the following paragraph. Four uniaxial strain-gauges with a resistance equal to 120 ohm and 6mm gage length have been installed on the aluminium panel (Figure 11).

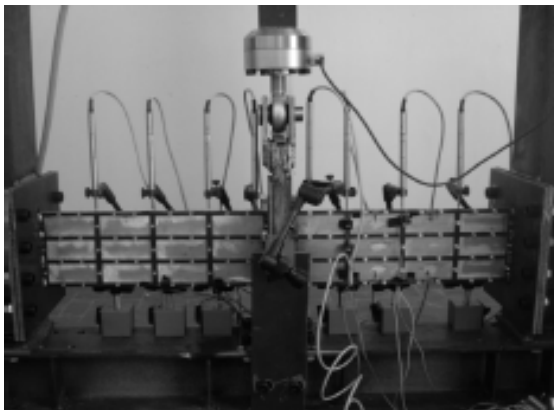

(a)

(b)

Figure 10. a) Displacement transducers LVDT installed on the panels; b) Load cell

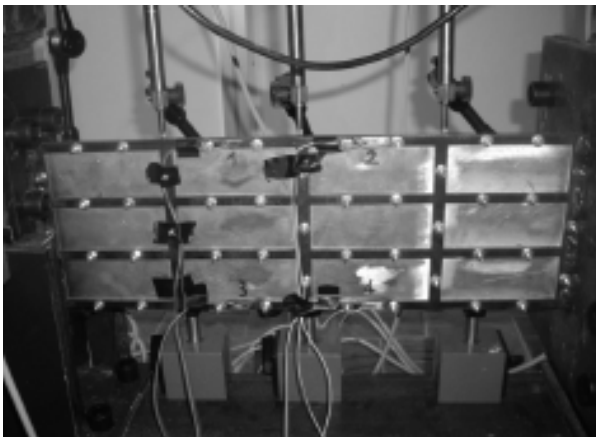

Figure 11. Positioning of uniaxial strain-gauges on the panel

## 6. Results of the Tests

The devices have been subjected to cycles of pulsating load from zero up to a maximum value increasing in positive and in negative direction. For higher cyclic loads the test has been performed only in one direction.

The test was over when the panels showed cracks at the welding of the base plate (Figure 12a). The crisis of the welding produced an out-of-plane instability of the device, as it is possible to observe in Figures 12b-c.

The results of the low-cycle tests could be synthesized in the load-displacement diagram shown in Figure 13.

(a) (b) (c)

Figure 12. Configuration at the end of the test: a) Crisis of the welding for the dissipater; b) and c) out-of-plane instability of the dissipator.

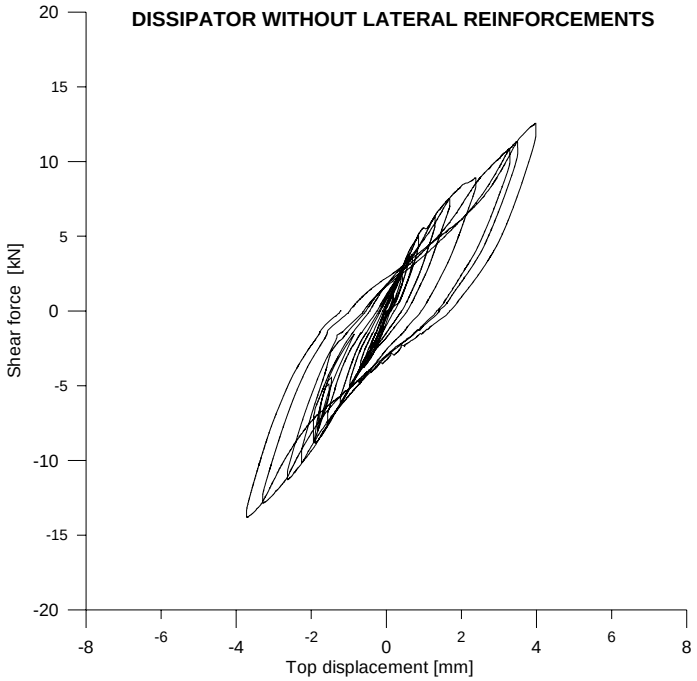


Figure 13. Experimental force-displacement diagram of the dissipator

The force-displacement plot shows that the area of hysteresis, corresponding to the energy dissipated by the device, is wide since the first cycles and it considerably increases as the level of the reached load increases. The origin of such dissipation lies in two prevailing phenomena:

- Friction between the steel and aluminium plates;
- Plasticization of the materials, presumably aluminium.

It is possible to plot the characteristic cyclic curve of the dissipator considering the peaks of each hysteresis cycle (Figure 14). Such characteristic curve represents the constitutive behavior of the panel that must be considered in the cases of a panel subjected to deformations repeated in the time, similarly to what happens during an earthquake. This curve puts in evidence what already previously stated regarding the hysteresis cycles: the panel shows on the whole a non-linear behaviour due to dissipative phenomena. Moreover, from this envelope plot it is possible to notice that the stiffness is lower than the one numerically obtained. This difference is evident if the two constitutive curves are plot on the same figure (Figure 15).

The experimental curve differs from the numerical one not only for the lower slope of the initial part, but also for the lower value of the transversal force reached in the non-linear part. Of course it is possible to find out the causes of these discrepancies. A first cause is due to the testing modalities and the elimination of the side plays existing in all the parts of the testing system, apart from the deformability of the frame utilized to load the devices. The second is due to a simplification introduced in the numerical model and that not necessarily is made in the real panel. Such a simplification has been considered in the FE model assuming the existence of a perfect joint between the steel plates and the aluminium plate that constitute the panel. In reality the load transmission is assured by the friction forces, by the bolts and by the obstacle constituted by the aluminium windows. Despite such forces, it is not possible to exclude the existence of micro-sliding between the plates that confer to the panel deformability higher than the one obtained from the numerical model.

Fundamental dynamic characteristics of velocity pulse sequences which resemble the near-fault ground motions are studied by using simplified combinational sinusoidal main-pulse and sub-pulse. The following conclusions can be drawn:

The spectral acceleration response in short periods is largely dependent with the duration of sub-pulse in the ground velocity. The velocity response and displacement response in short periods are also dependent with the duration of sub-pulse; however, the influences of sub-pulse have a reducing trend comparing with the influences on the spectral acceleration response. The peak spectral displacement response may occur not in the resonance bond, but occurs when the structural period far exceeds main-pulse duration for the case of a main-pulse with a short enough

duration sub-pulse. The maximum acceleration amplification effect in short periods may be caused by the sub-pulse with short duration. The decay of sub-pulse duration causes the periods corresponding to peak acceleration response and maximum acceleration amplification effect to shift to shorter periods.

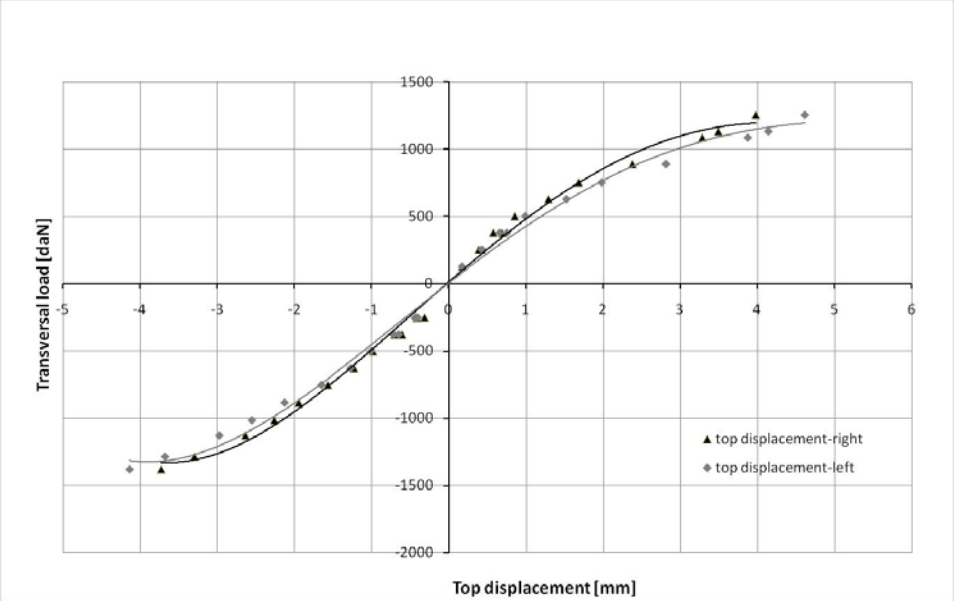


Figure 14. Cyclic curve envelope: constitutive behavior of the dissipating device

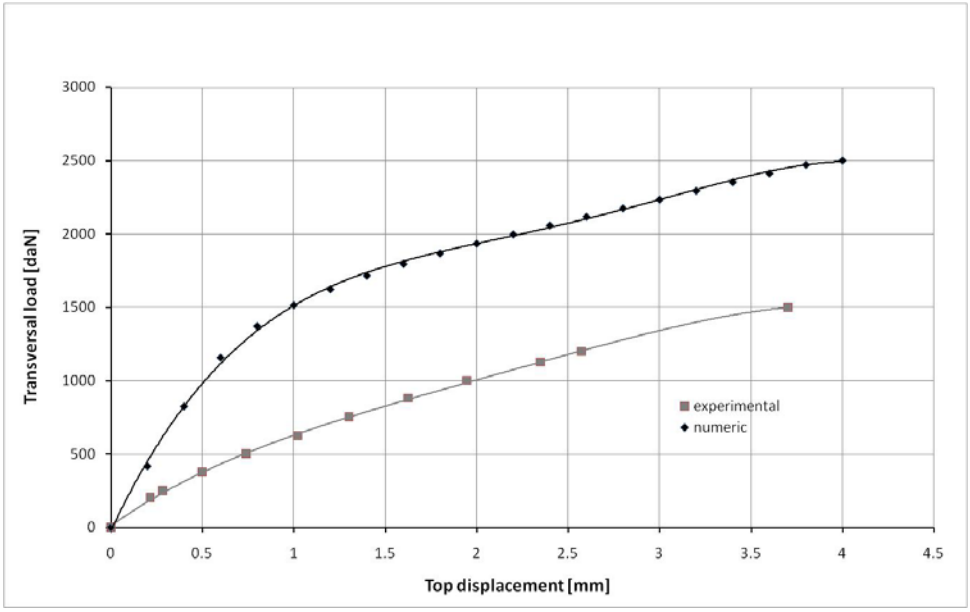


Figure 15. Comparison between the numerical and experimental behavior of the device with lateral reinforcements

As shown in this study, the responses of structure are directly related with the main-pulse, sub-pulse, and their relations. This triggers us to reconsider the capacity of approximation by a simple wave with equal main-pulse and sub-pulse duration and amplitude. Perhaps a pulse sequence is a better choice.

## 7. Conclusions

In the present paper a hysteretic dissipator made of aluminium and steel has been conceived and designed. A numerical optimization technique has been used to choose the better geometrical configuration of the device. Moreover the change of the dynamic properties of a frame equipped with the proposed device and subjected to a selected set of earthquakes has been evaluated. Finally, static mechanical characterization of the panel has been carried out through an appropriate experimental set-up.

The panel design and the numerical evaluation of the dynamic properties of a frame suggested the efficacy of the proposed device against the protection of structures subjected to earthquakes. The results of the characterization tests have put in evidence a hysteretic behavior with energy dissipation. The comparison between the experimental and numerical constitutive behaviors shows that the real panel is much more deformable that the one obtained from the numerical study. Such a difference is due to the unavoidable elimination of the side plays phenomena and to the not perfect adherence of the aluminium and steel plates constituting the device. From the point of view of the numerical modelling, the model should be improved introducing the friction existing between the plates.

In the future the building details of the dissipator could be improved to enlarge its field of use, increasing the maximum excursion, the maximum displacement and the maximum number of cycles before failure of the device.

## Acknowledgements

This study has been supported by the ReLuis Consortium, Research Line n. 7: “Isolation Technologies for the Control of Structures and Life-lines”.

## References

De Matteis, G., Mazzolani, F.M. and Panico, S.:(2007), “Pure aluminium shear panels as dissipative devices in moment-resisting steel frames”, *Earthquake Engineering and Structural Dynamics*, Vol. 36, No. 7, Pages 841-859.

Diaferio, M., Foti, D. and Nobile R.(2008), "Design optimization of aluminium-steel devices for passive protection of structures", *4th Conference on Structural Control (ECSC2008),* St. Petersburg, Russia, Paper No 136.

Foti, D. and Diaferio, M. (1999), "Shear panels for seismic protection of buildings", *4th European Conference of Structural Dynamics–EURODYN'99,* Prague, Republic of Czech.

Foti, D., Nobile, R.(2000), "Characterization tests of new aluminium and steel energy dissipating devices", *5th International Conference on Computational Structures Technology*: *Identification, Control and Optimisation of Engineering Structures*, Civil-Comp Press, Leuven, Belgium.

Gattulli, V., Lepidi, M., and Potenza, F. (2007), "Identifcation of analytical and finite element model for the Jetpacs three-dimensional frame", *Jetpacs Report No. 2, Research Project No. 7 of 2005-2008 ReLuis Project*, Naples, Italy.

Nakashima, M., Iwai, S., Iwata, M., Takeuchi, T., Konomi, S., Akazawa, T. and Saburi, K. (1994), "Energy dissipation behavior of shear panels made of low yield steel", *Earthquake Engineering and Structural Dynamics*, Vol. 23, No. 12, Pages 1299-1313.

Nakashima, M. (1995), "Strain-hardening behavior of shear panels made of low-yield steel. I: Test", *ASCE: Journal of Structural Engineering*, Vol. 121, No. 12, Pages 1742-1749.

Ponzo, F.C., Cardone, D., Di Cesare, A., Moroni, C., Nigro, D. and Vigoriti, G. (2007), "Dynamic tests on Jetpacs steel frame experimental model set up", *Jetpacs Report No. 3, Research Project No. 7 of 2005-2008 ReLuis Project*, Naples, Italy.

Rai, D.C. and Wallace, B. J. (1998), "Aluminium shear-link for enhanced seismic resistance", *Earthquake Engineering and Structural Dynamics*, Vol. 27, No. 4, Pages 315-342.

Serino, G., Chandrasekaran, S., Marsico, M.R. and Spizzuoco, M. (2007), "Description and analytical modeling of the Jetpacs steel frame prototype" *Jetpacs Report No. 1, Research Project No. 7 of 2005-2008 ReLuis Project*, Naples, Italy.

Yamaguchi, T., Takeuchi, T., Nagao, T., Suzuki, T., Nakata, Y., Ikebe, T. and Minami, A. (1998), "Seismic control devices using low-yield-point steel", *Nippon Steel Technical Report No. 77*, Nippon Steel Corporation, Chiba, Japan, Pages 65-72.